

# ALGORITHM TO ANALYZE COMPLEX MAGNETIC STRUCTURES USING A TUBE APPROACH

B. Riemann\*, M. Aiba  
Paul Scherrer Institut, 5232 Villigen PSI, Switzerland

## Abstract

Modern synchrotron light sources often require sophisticated multipole field distributions that need to be realized by complex magnet structures. To pre-validate these magnet structures in simulation, the extraction procedure needs to output standard multipoles as well as fringe effects. The approach presented in this manuscript uses a volumetric grid map of the magnetic flux density as input. After computation of the reference trajectory (leapfrog integration), a large linear system is solved to compute transverse polynomial coefficients of the magnetic scalar potential in a series of interconnected thin cylinders (linear basis functions) along with that reference. The import of these coefficients into a lattice simulation is discussed using a modification of the tracking code `tracy`. The shown approach is routinely used to check models of SLS 2.0 magnets for their properties.

## INTRODUCTION

Analysis of 3d magnetic fieldmaps can be done by several means, the most prevalent being direct import and interpolation. However, it can be useful to import multipole fields in a manner similar to the standard idealized magnet types used in accelerator lattices. To do this, the design trajectory through the field must be computed, and polynomial coefficients of the field around this trajectory must be found. While this task seems straightforward, it is non-trivial to obtain robust polynomial coefficients around a curved trajectory even from an equidistant volumetric grid. In the following, we go through the basic steps of such a fitting technique, collecting field points in a “tube” around the curved design trajectory. The procedure takes some inspiration from [1], where the fitting of polynomials is briefly mentioned, and can also be related to undulator studies in the machine plane [2].

## REPRESENTATION

Cartesian magnet coordinates are defined as  $X, y, Z$  in the following, with  $Z$  having only small angles with the beam path  $s$ , and the direction of  $y$  being perpendicular to the machine plane  $X - Z$ . For simplicity, the reference trajectory will be assumed to be in the machine plane, so that the beam  $y$  coordinate and the magnet coordinate are identical.

The inputs available for our computation are magnetic flux density vectors  $\vec{B}^{(i)}$  on a grid of points  $X_i, y_i, Z_i$ . For all following computations, we rescale  $\vec{B}$  to units of curvature with beam rigidity  $B\rho = p/q$ ,

$$\vec{b}^{(i)} = \vec{B}^{(i)} / (B\rho).$$

\* <https://orcid.org/0000-0002-5102-9546>

## MACHINE PLANE TRAJECTORY

The machine plane trajectory can be parameterized with coordinates  $Z(s), X(s)$ . The curvature vectors in this plane are interpolated using bivariate splines [3, 4] to obtain a continuous curvature map  $b_y(Z, X)$ . With this map, we use the same coordinate system as in [5] so that

$$\frac{d}{ds} \begin{pmatrix} Z \\ X \end{pmatrix} = \begin{pmatrix} \cos \theta(s) \\ -\sin \theta(s) \end{pmatrix}, \quad \frac{d\theta}{ds} = b_y(Z, X).$$

The approximated orbit with step size  $\Delta s$  starts at  $Z_0 = 0, X_0$  and is mirror-symmetric in  $Z$ ; the first line segment has  $\theta_0 = b_y(0, X_0) \Delta s/2$ . From these initial conditions, the leap-frog scheme is employed to construct the trajectory to a given length. Afterwards, averaged tangent vectors

$$n_{Z,j} = \cos \tilde{\theta}_j, \quad n_{X,j} = -\sin \tilde{\theta}_j \quad \text{with} \quad \tilde{\theta}_j = \frac{\theta_{j-1} + \theta_j}{2}$$

can be constructed. For each trajectory point  $j \in \{0, \dots, J-1\}$  one can define a transverse plane normal to this tangent vector. All changes in particle momentum are applied in these planes.

## 3D ANALYSIS AND GENERAL MULTIPOLES

The flux density in the beam pipe, and thus  $\vec{b}(X, y, Z)$ , is curl- and divergence-free, and one can define  $\Omega$  with

$$\vec{b}(X, y, Z) = \vec{\nabla} \Omega(X, y, Z) \quad \text{and} \quad \Delta \Omega = 0.$$

**Cylinder approach** For each aforementioned transverse plane, the field on that plane can be projected into that plane. The projected field is defined using only in-plane values of  $\Omega$ , parameterized as  $\tilde{\Omega}_j(x, y)$ ,

$$\tilde{b}_x^{(j)}(x, y) = \frac{d\tilde{\Omega}_j(x, y)}{dx}, \quad \tilde{b}_y^{(j)}(x, y) = \frac{d\tilde{\Omega}_j(x, y)}{dy}. \quad (1)$$

While these projected fields are still curl-free, they can possess in-plane divergence  $\Delta_{xy} \tilde{\Omega} \neq 0$ , giving rise to fringe effects. Therefore  $\tilde{\Omega}$  needs to be parameterized as a general 2d function (see Fig. 1). For tracking purposes, we can just use a standard 2d polynomial up to order  $M$

$$\tilde{\Omega}_j(x, y) = \sum_{pq} \Psi_{j pq} x^p y^q \quad \text{with} \quad 0 < p + q \leq M. \quad (2)$$

Note that as we are using machine-plane symmetry, the  $\Psi$  coefficients for even  $q$  must vanish.

To find the  $\Psi$  coefficients, one can select all  $\vec{b}^{(i)}$  input vectors located in a thin cylinder of height  $\Delta s$  and radius  $R$ ,

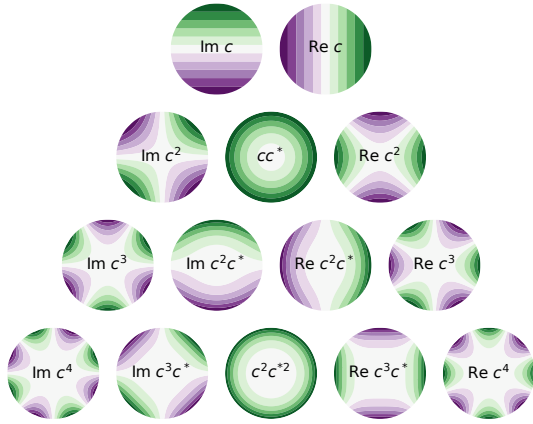


Figure 1: Alternative 2d basis functions for  $\tilde{\Omega}$  using a complex number  $c = x + iy$ , inspired by [6] and Zernike polynomials. Left and right edges of the triangle show standard upright and skew multipoles, which have no in-plane divergence. The interior maps fringe-like effects. In magnets with machine-plane symmetry, only “Im” entries occur.

its center located in the respective trajectory point  $(X_j, Z_j)$ , and its base parallel to the plane.  $R$  is chosen to be close to the vacuum chamber radius, ensuring only valid in-vacuum points are considered while also allowing robust convergence.

Following steps are performed independently for each trajectory point or cylinder  $j$ . The curvature applied to the trajectory is subtracted from the field vectors. Then, they are transformed to the  $\tilde{b}_x, \tilde{b}_y$  components of the transverse plane, including the projection of the grid to beam coordinates  $X_i, Z_i \rightarrow x_i$  (unmodified  $y_i$ ), and used for fitting with Eqs. (1) and (2) while excluding the curvature term  $\Psi_{j01}$ .

**Tube approach** While aforementioned approach works in principle, it can be insufficient when fields are changing significantly fast (in  $\sim \Delta s$ ) in longitudinal direction. A solution is to employ linear basis functions in this direction. We assume a potential in beam coordinates

$$\tilde{\Omega}(x, y, s) = \sum_{j=0}^{J-1} \tilde{\Omega}_j(x, y) T\left(\frac{s-j\Delta s}{\Delta s}\right),$$

where  $T(\chi)$  denotes the triangle function with non-zero values for  $\chi \in ]-1, 1[$ . This potential can also be used to obtain all  $\Psi$  coefficients. Again only field points inside a “tube” around the reference orbit with radius  $R$  are valid. The valid vectors  $\tilde{b}^{(i)}$  are transferred to the respective transverse planes  $\tilde{b}_x^{(i)}, \tilde{b}_y^{(i)}$ , and their grid locations transform  $X_i, Z_i \rightarrow x_i, s_i$  ( $y_i$  unchanged). Then, we obtain a linear system for the yet unknown polynomial coefficients  $\Psi_{j pq}$  as

$$\begin{aligned} \tilde{b}_x^{(i)} &= \sum_{j pq} \Psi_{j pq} p x_i^{p-1} y_i^q T\left(\frac{s_i-j\Delta s}{\Delta s}\right), \\ \tilde{b}_y^{(i)} &= \sum_{j pq} \Psi_{j pq} q x_i^p y_i^{q-1} T\left(\frac{s_i-j\Delta s}{\Delta s}\right), \end{aligned} \quad (3)$$

involving all valid fieldmap points  $i$ , and all trajectory points  $j$  (at  $s = j\Delta s$ ). This system (sparsity  $\sim 1 - 2/J$ ) can be solved using least-square solvers for sparse matrices [4].

## EXAMPLES

To demonstrate the basic workings of the algorithm, we generate four sets of 3d curvature maps. As first examples, we begin with fields independent of the  $Z$  coordinate.

The most elementary field is a homogenic vertical field in the machine plane, leading to the coefficients shown in Fig. 2. As expected, all coefficients besides the linear increasing bending angle vanish in numerical noise.

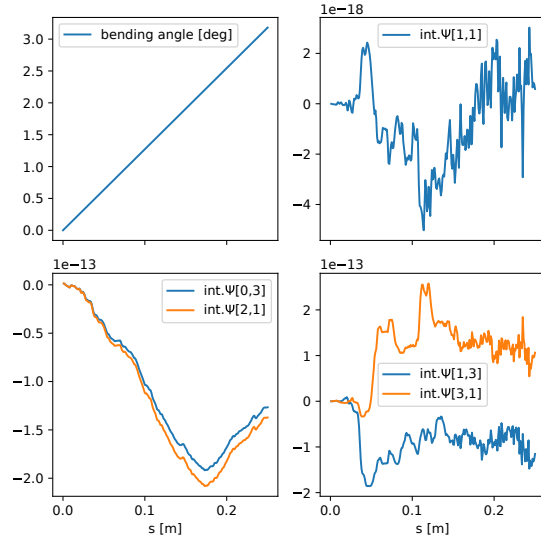


Figure 2: Cumulative integral of polynomial coefficients of homogenic vertical field. The curves  $\text{int.}\Psi[p, q]$  hold the coefficients  $\Psi_{j pq}$  cumulatively integrated in  $s_j$  using trapezoid rule. From top left to bottom right: bending angle, quadrupole coefficient, (both upright) sextupole polynomial coefficients, octupole coefficients.

A similar situation occurs for the homogenic quadrupole. Naturally, all coefficients besides the quadrupole coefficient should be negligible, as can be observed in Fig. 3.

**Square-wave synthesis of edge fields** To model magnet edges at position  $Z = \pm L/2$ , we require a smooth function resembling a square wave of period length  $2L$ . We choose  $L = 0.25$  m and the function

$$S(z) = \frac{8}{9} + \cos(\kappa_1 z) - \frac{1}{9} \cos(\kappa_3 z) \quad \text{with } \kappa_n = n \frac{\pi}{L}. \quad (4)$$

For a quadrupole with edge, we can synthesize the following potential that will fulfill the Laplace equation

$$\Omega(X, y, Z) = \sum_n 4a_n \frac{\cos(\kappa_n Z) I_2(\kappa_n r) \sin(2\phi)}{\kappa_n^2},$$

with the cylinder coordinates  $r = \sqrt{X^2 + y^2}$  and  $\phi = \arctan2(Y, x)$ . The  $n = 0$  summand reduces to  $a_0 X y$ . Using Eq. (4) we insert the terms for  $a_n$  to obtain the potential,

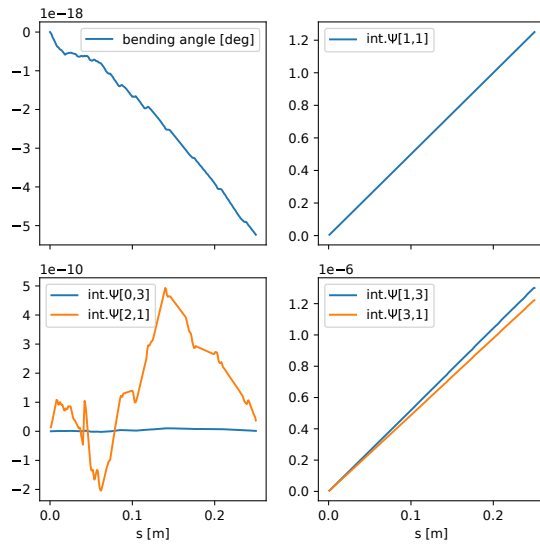


Figure 3: Cumulative integral of polynomial coefficients of homogenic quadrupole. See Fig. 2 for legend.

generating the 3d map using  $\vec{b} = \vec{\nabla}\Omega$ . This map is used as input for the Tube algorithm. In addition to the quadrupolar field distribution, we can expect octupole and higher-order edge effects consistent with quadrupole symmetry. The octupole component can be observed in Fig. 4 - as quadrupole symmetry is consistent with  $x, y$  interchange, the octupole components (1,3) and (3,1) overlap.

For a **dipole with edge**, a  $2L$ -periodic solution to the Laplace equation for looks like

$$\Omega(y, Z) = \sum_n a_n \frac{\cos(\kappa_n Z) \sinh(\kappa_n y)}{\kappa_n}$$

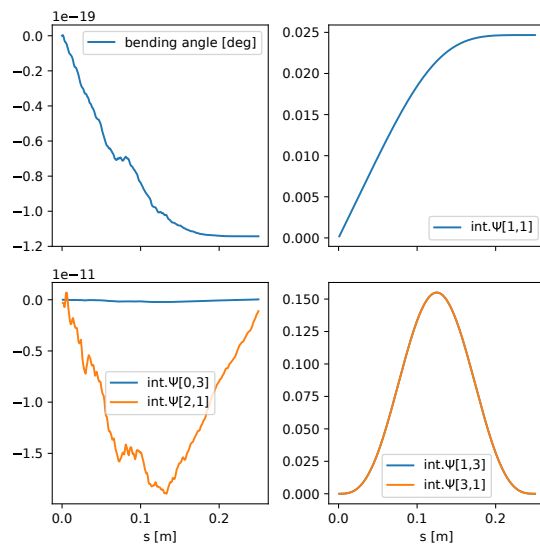


Figure 4: Cumulative integral of polynomial coefficients of quadrupole with edge. See Fig. 2 for legend.

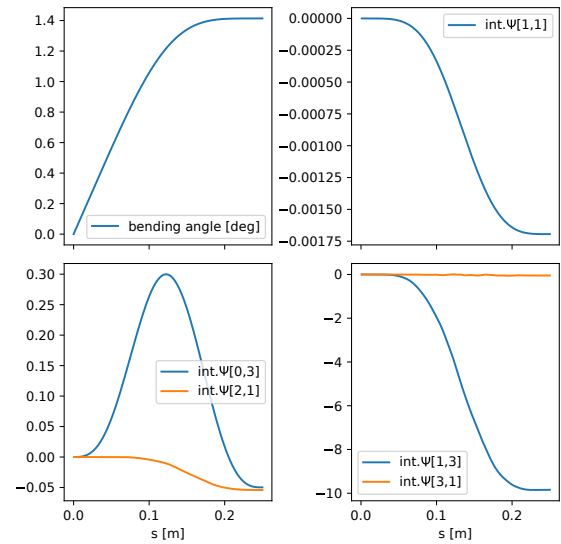


Figure 5: Cumulative integral of polynomial coefficients of dipole with edge. See Fig. 2 for legend.

The  $n = 0$  summand reduces to  $a_0 y$ . The  $a_n$  values are again taken from (4). The  $\Psi_{j pq}$  coefficients are shown in Fig. 5. As expected, bending reduces at the edge. We can observe edge focusing as shown by the quadrupole term (1,1). There is also a sextupolar fringe effect – it can be observed that this field contribution is not a standard sextupole, as the sextupole potential coefficients  $y^3$  and  $x^2 y$ , represented by (0,3) and (2,1) are not proportional to each other. The  $y^3$  term originates from the Taylor series of  $\sinh(\kappa_n y)$ , while the  $x^2 y$  term occurs due to the edge angle, mixing in the  $d^2 b_y / dZ^2$  term. The fringe effect also extends to octupolar terms,  $xy^3$  being caused by a combination of the sinh series and edge-angle mixing of  $db_y / dZ$ .

## CONCLUSION

The presented algorithm is a part of the checking routine for combined-function magnets of the Swiss Light Source upgrade (SLS 2.0), investigating their effects on linear and nonlinear optics. For this, a fork of the well-known tracking code tracy [7] is employed, allowing us to include the aforementioned generalized multipoles (polynomials) into the standard TPSA procedure. We can circumvent interpolation of fieldmaps during tracking as well as ensure vanishing curl. Note that this method can be adapted to vacuum chambers with arbitrary shape by changing the cross section of the tube. Also, irregular volumetric field data is supported in the tube approach, if a start reference trajectory is known.

## ACKNOWLEDGMENTS

The authors thank M. Negrazus, C. Calzolaio, V. Vrankovic, S. Bettoni, M. Boege and A. Streun for interesting discussions.

## REFERENCES

- [1] S. Machida and E. Forest, “Beam optics and dynamics of FFAG accelerators”, in *Proc. 16th Int. Conf. Cyclotrons*, East Lansing, USA, 2001. pp. 204-207. doi:10.1063/1.1435234
- [2] S. Bettoni, “Reduction of the integrated odd multipoles in periodic magnets”, *Phys. Rev. ST Accel. Beams*, vol. 10, no. 4, p. 042401, 2007. doi:10.1103/PhysRevSTAB.10.042401
- [3] P. Dierckx, *Curve and Surface Fitting with Splines*, NY, USA, Oxford University Press, 1993.
- [4] P. Virtanen, R. Gommers, T. E. Oliphant, *et al.*, “SciPy 1.0—Fundamental Algorithms for Scientific Computing in Python”, 2019. doi:10.1038/s41592-019-0686-2
- [5] M. Aiba, M. Boege, M. Ehrlichman, and A. Streun, “Magnetic field of longitudinal gradient bend”, *Nucl. Instrum. Methods Phys. Res. A*, vol. 892, pp. 41-47, 2018. doi:10.1016/j.nima.2018.02.111
- [6] Orthopy, <https://github.com/nschloe/orthopy>
- [7] Tracy tracking code, <https://github.com/jbengtsson/tracy-3.5>